Molecular Dynamics in Mouse Atrial Tumor Sarcoplasmic Reticulum

John C. Voss,* James E. Mahaney,* Larry R. Jones,‡ and David D. Thomas*
*Department of Biochemistry, University of Minnesota Medical School, Minneapolis, Minnesota 55455, and ‡Department of Medicine, Krannert Institute of Cardiology, Indiana University School of Medicine, Indianapolis, Indiana 46202 USA

ABSTRACT We have determined directly the effects of the inhibitory peptide phospholamban (PLB) on the rotational dynamics of the calcium pump (Ca-ATPase) of cardiac sarcoplasmic reticulum (SR). This was accomplished by comparing mouse ventricular SR, which has PLB levels similar to those found in other mammals, with mouse atrial SR, which is effectively devoid of PLB and thus has much higher (unregulated) calcium pump activity. To obtain sufficient quantities of atrial SR, we isolated the membranes from atrial tumor cells. We used time-resolved phosphorescence anisotropy of an erythrosin isothiocyanate label attached selectively and rigidly to the Ca-ATPase, to detect the microsecond rotational motion of the Ca-ATPase in the two preparations. The time-resolved phosphorescence anisotropy decays of both preparations at 25°C were multi-exponential, because of the presence of different oligomeric species. The rotational correlation times for the different oligomers were similar for the two preparations, but the total decay amplitude was substantially greater for atrial tumor SR, indicating that a smaller fraction of the Ca-ATPase molecules exists as large aggregates. Phosphorylation of PLB in ventricular SR decreased the population of large-scale Ca-ATPase aggregates to a level similar to that of atrial tumor SR. Lipid chain mobility (fluidity), detected by electron paramagnetic resonance of stearic acid spin labels, was very similar in the two preparations, indicating that the higher protein mobility in atrial tumor SR is not due to higher lipid fluidity. We conclude that PLB inhibits by inducing Ca-ATPase lateral aggregation, which can be relieved either by phosphorylating or removing PLB.

INTRODUCTION

The Ca-ATPase of the sarcoplasmic reticulum (SR) is a 110-kDa transmembrane protein, which couples the hydrolysis of ATP to the active transport of calcium ions into the SR lumen against a concentration gradient (reviewed by Inesi, 1985). In cardiac SR, the Ca-ATPase is regulated by phospholamban (PLB), which is not found in fast-twitch skeletal SR (Kirchberger and Tada, 1976; Tada and Katz, 1982; Jorgensen and Jones, 1986; Voss et al., 1994). Phospholamban is an amphipathic, 52-residue protein, with a hydrophilic (cytoplasmic) phosphorylation domain and a hydrophobic (transmembrane) domain, which probably exists as a homopentamer (Wegener et al., 1986; Simmerman et al., 1986; Fujii et al., 1987). Phosphorylation of PLB results in a stimulation of ATPase activity and calcium uptake at submicromolar [Ca^{2+}] (Davis et al., 1983; Tada et al., 1988). Studies using reconstitution of the Ca-ATPase and PLB (Inui et al., 1986), proteolytic cleavage of the cytoplasmic portion of PLB (Kirchberger et al., 1986), and co-expression of the Ca-ATPase and PLB in COS-1 cells (Fujii et al., 1990; Toyofuku et al., 1993) and Sf21 insect cells (Autry et al., 1994) provide strong evidence that unphosphorylated PLB is a Ca-ATPase inhibitor at low [Ca^{2+}]. Evidence has been provided that PLB's inhibitory action involves 1) interaction between the cytoplasmic domain of PLB and sites in the phosphorylation domain and nucleotide-binding hinge domain of the Ca-ATPase (Toyofuku et al., 1993), and 2) electrostatic interaction between the basic (positively charged) residues of PLB's cytoplasmic domain and negatively charged residues in the stalk region of the Ca-ATPase (Voss et al., 1994; Tada et al., 1989). The regulation of the Ca-ATPase by PLB shows an electrostatic dependence consistent with a major involvement of charged residues (Xu and Kirchberger, 1989; Chiesi and Schwaller, 1989).

Extensive spectroscopic studies of the Ca-ATPase in rabbit skeletal SR have shown that the molecular dynamics of the enzyme and its associated lipids are important for the Ca-ATPase mechanism (Thomas and Mahaney, 1993; Thomas and Karon, 1994). For example, decreased ATPase activity results from perturbations that decrease microsecond protein rotational motion detected by saturation transfer electron paramagnetic resonance (ST-EPR) (Squier and Thomas, 1988; Squier et al., 1988a, b; Mahaney and Thomas, 1991). Similarly, time-resolved phosphorescence anisotropy (TPA) measurements show a strong correlation between conditions that inhibit (or increase) Ca-ATPase activity and those that promote protein association (dissociation), including some perturbations that have negligible effects on lipid fluidity (Birmachu and Thomas, 1990; Voss et al., 1991; Karon and Thomas, 1993).

We have previously compared Ca-ATPase rotational dynamics in dog cardiac and rabbit skeletal SR (Birmachu et al., 1993). The rotational mobility of the enzyme in cardiac SR was much more restricted than the enzyme in skeletal SR. Our results indicated that the decreased mobility of the

Received for publication 8 September 1994 and in final form 17 February 1995.

Address reprint requests to Dr. David D. Thomas, Department of Biochemistry, University of Minnesota Medical School, Millard 4-225, 435 Delaware Street SE, Minneapolis, MN 55455. Tel.: 612-625-0957; Fax: 612-624-0632; E-mail: ddt@ddt.biochem.umn.edu.

Abbreviations used: SR, sarcoplasmic reticulum; MVSR, mouse ventricular SR; MASR, mouse atrial tumor SR; TPA, time-resolved phosphorescence anisotropy; EPR, electron paramagnetic resonance; ErITC, erythrosin-5-isothiocyanate; SASL, stearic acid spin label; MOPS, 3-(*N*-morpholino)-propanesulfonic acid.

0006-3495/95/05/1787/09 $2.00

cardiac enzyme could not be attributed to differences in lipid composition or bilayer fluidity, but was almost certainly due to a large fraction of the enzyme in cardiac SR associated in large-scale aggregates. Based on previous studies correlating changes in Ca-ATPase aggregation with changes in Ca-ATPase mobility and activity (reviewed by Thomas and Mahaney, 1993), the high level of protein association and lower Ca-ATPase activity in cardiac SR relative to skeletal SR was attributed to the presence of PLB in the cardiac membrane (Birmachu et al., 1993). We have investigated recently the Ca-ATPase dynamics in cardiac SR as a function of PLB phosphorylation and [Ca^{2+}] (Voss et al., 1994). This work showed that the cardiac Ca-ATPase is highly aggregated in its inhibited state, when PLB is unphosphorylated at submicromolar Ca^{2+}, but stimulation of the Ca-ATPase, either by PLB phosphorylation or micromolar [Ca^{2+}], correlates with enzyme dissociation from large aggregates.

To test directly the functional and physical effects of PLB on the Ca-ATPase, it is desirable to study the cardiac enzyme in its native membrane in the presence and absence of PLB. Jones and Field (1993) have reported that cardiac SR vesicles isolated from AT-1 cardiomyocytes are essentially devoid of PLB, whereas mouse ventricular SR vesicles contain high levels of PLB. AT-1 cardiomyocytes are a transplantable tumor lineage derived from transgenic mice expressing the SV40 large T antigen (Field, 1988). Large amounts of mouse atrial SR vesicles sufficient for direct physical study are easily isolated from these subcutaneously growing tumors. Therefore, in the present study, we have used TPA to characterize the microsecond protein rotational motion of the Ca-ATPase in mouse ventricular SR and mouse atrial tumor SR (obtained from AT-1 cells), to compare directly the enzyme mobility in these two systems, and thus to determine directly the effects of PLB on Ca-ATPase dynamics and protein-protein association. Because protein rotational diffusion can be affected either by protein structure or by lipid viscosity (Saffman and Delbrück, 1975), we have also used EPR spectroscopy to measure lipid chain rotational dynamics in the two systems. The absence of PLB in atrial SR and the presence of PLB in ventricular SR allows for the precise determination of the effects of PLB on the molecular dynamics of the cardiac Ca-ATPase of the same isoform in the same membrane from the same species.

MATERIALS AND METHODS

Reagents and solutions

Erythrosin 5-isothiocyanate (ErITC) was obtained from Molecular Probes Inc. (Eugene, OR) and was stored in DMF at −70°C. Glucose oxidase type IX, catalase, glucose, and ATP were obtained from Sigma Chemical Co. (St. Louis, MO). Calyculin A (phosphatase inhibitor) was obtained from LC Services Corporation (Woburn, MA). Fatty acid spin labels were obtained from Aldrich Chemical Company (Milwaukee, WI). All other reagents were of the highest purity available. Biochemical and spectroscopic measurements were carried out in a solution containing 60 mM KCl, 1 mM $MgCl_2$, 10 mM EGTA, 2 mM $CaCl_2$ (0.1 μM free Ca^{2+}) (Fabiato, 1988), 50 mM MOPS, pH 7.0, 25°C.

SR Vesicle isolation

The mouse atrial tumor and ventricular SR membranes used in this study were identical to those isolated and characterized by Jones and Field (1993). The isolation procedure was based on Jones and Cala (1981). Briefly, atrial tumors from two mice (approximately 20 g of tissue each) or 110 mouse ventricles (approximately 15 g of tissue) were homogenized 3 times for 30 s in 10 mM $NaHCO_3$ with a Polytron. SR vesicles were collected as the membranes sedimenting at 45,000 × g_{max} for 30 min. After extraction with 0.6 M KCl, 30 mM histidine, pH 7.0, the vesicles were pelleted by centrifugation at 45,000 × g_{max} for 30 min and resuspended in 0.25 M sucrose, 30 mM histidine, pH 7.2. The vesicles were frozen in small aliquots and stored at −40°C until use. Protein concentrations were determined by the method of Lowry et al. (1951) using BSA as a standard.

SDS gels and immunoblotting

SDS-PAGE was performed according to the method of Jones et al. (1985) using an 8% slab gel, 1.5 mm thick. The specificity of ErITC labeling of the Ca-ATPase was confirmed using quantitative analysis of the photographic negatives of SDS gels of SR labeled with FITC. Gels were illuminated with a UV lamp, and photographs were taken through a 550-nm cutoff filter, before staining the gels with Coomassie blue, as described previously (Birmachu et al., 1993). FITC was used in the label specificity studies in place of ErITC because FITC fluoresces much more intensely than ErITC, allowing visualization of the label distribution in the fluorescent photographs. ErITC is nearly identical chemically to FITC, and inhibits both the rabbit skeletal and dog cardiac isoforms of the Ca-ATPase in a manner similar to that of FITC (Birmachu et al., 1993), strongly suggesting that ErITC derivatizes primarily the FITC site of the enzyme. Immunoblotting was performed as described by Jones and Field (1993) using the Ca-ATPase monoclonal antibody 2A7-A1 and the PLB monoclonal antibody 2D12. Antibody-reacting bands were detected by autoradiography after incubation with ^{125}I-labeled protein A (Manalan and Jones, 1982), and quantified with the use of a Bio-Rad GS-250 Molecular Imager. Autoradiography of ^{32}P-containing SDS gels was performed according to the method of Voss et al. (1994).

The amount of Ca-ATPase protein in the mouse atrial tumor and ventricular SR preparations was approximately 17 and 26% of the total protein, respectively, determined from densitometry scans of the Coomassie blue-stained SDS polyacrylamide gels. To increase the Ca-ATPase purity in the atrial tumor SR vesicles to a level comparable with ventricular SR, the crude atrial tumor SR vesicles were loaded onto a discontinuous (25, 35, 40, and 50%) sucrose gradient (in 20 mM MOPS, 150 mM KCl, pH 7.2) and centrifuged for 10 h at 25,000 rpm in a Beckman SW-28 rotor. The vesicles that migrated to the 35–45% sucrose interface were harvested and pelleted at 45,000 × g_{max} for 30 min and resuspended in 0.25 M sucrose, 30 mM histidine, pH 7.2. The Ca-ATPase protein in the purified atrial tumor SR vesicles comprised approximately 25% of the total protein (Fig. 1).

Quantitative immunoblotting was used in combination with SDS gel electrophoresis to determine the relative ratio of PLB to Ca-ATPase in the two SR preparations (Fig. 1). The two preparations contain similar amounts of Ca-ATPase (ventricular SR/atrial tumor = 1.13). However, the ventricular SR preparation contains 7 times more PLB than does the atrial tumor SR preparation, so the PLB/Ca-ATPase ratio is 6.2 times greater in mouse ventricular SR than in mouse atrial tumor SR.

Labeling and sample preparation

For phosphorescence experiments, the SR vesicles were labeled with ErITC, as described previously (Birmachu and Thomas, 1990). This procedure specifically labels the Ca-ATPase in both skeletal and cardiac SR (Birmachu et al., 1993). However, extensive studies with skeletal SR labeled at this site with FITC show that the enzyme is otherwise unperturbed, has normal calcium binding, and goes through the normal calcium-pumping enzymatic cycle with less bulky substrates such as acetyl phosphate (Teruel and Inesi, 1988). Therefore, the conformational and rotational dynamics of FITC-SR

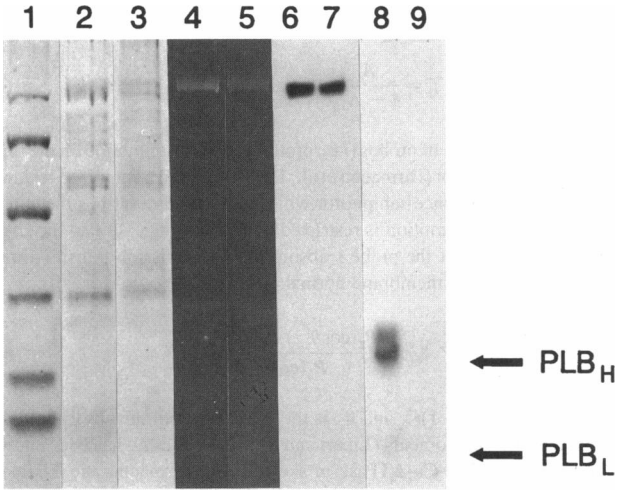

FIGURE 1 SDS gel electrophoresis and autoradiographs of immunoblots of optically labeled mouse ventricular SR and mouse atrial tumor SR. Samples were labeled as described in the text. Lane 1 shows Coomassie blue-stained protein molecular weight standards. Coomassie blue-stained bands of ErITC-labeled ventricular and atrial tumor SR are shown in lanes 2 and 3, respectively. Photographs of the fluorescent bands of FITC-labeled ventricular and atrial tumor SR are shown in lanes 4 and 5, respectively. Lanes 6 and 7 show immunoblots detecting the Ca-ATPase in mouse ventricular and atrial tumor SR, respectively, with SERCA2-specific monoclonal antibody 2A7-A1. Lanes 8 and 9 show immunoblots of PLB in mouse ventricular and atrial tumor SR, respectively, with the monoclonal antibody 2D12. PLB_H and PLB_L denote the pentameric and monomeric forms of PLB, respectively. Note the negligible presence of PLB in atrial tumor SR in lane 9. Molecular mass standards are: phosphorylase B (97.4 kDa), BSA (66.2 kDa), ovalbumin (45 kDa), carbonic anhydrase (31 kDa), soybean trypsin inhibitor (21.5 kDa), and lysozyme (14.4 kDa).

and ErITC are probably representative of the unlabeled protein. Labeled samples were kept on ice and used the same day for spectroscopic measurements.

The stoichiometry of labeling was 0.8 ± 0.1 moles of ErITC bound per ATPase in both the atrial and ventricular SR, determined by measuring the absorbance at 536 nm of an aliquot of ErITC-SR in the presence of 2% deoxycholate, using ϵ_{536} = 80,000 M^{-1} cm^{-1} for the *Ca-ATPase-bound* ErITC (Birmachu and Thomas, 1990) and assuming a molecular mass of 110 kDa for the Ca-ATPase. Densitometer scans of the fluorescent and Coomassie blue-stained SDS polyacrylamide gels (Fig. 1) showed that the probe binds specifically to the Ca-ATPase in both the atrial and ventricular SR, because 68 ± 3 and 65 ± 3% of the fluorescence intensity was associated with the 110-kDa ATPase band in both atrial and ventricular SR, respectively. The remaining fluorescence intensity in each sample was localized at the top of the gel, which we determined by Western blot analysis (not shown) was Ca-ATPase that did not enter the gel. The specificity of labeling, therefore, was similar to that obtained for rabbit skeletal ErITC-Ca-ATPase, where the label reacts with >90% specificity with Lys 515 in the Ca-ATPase (Mitchinson et al., 1982; Birmachu et al., 1993), and the extent of labeling was nearly identical in the mouse atrial tumor SR and mouse ventricular SR preparations.

Lipid hydrocarbon chain rotational mobility was measured with stearic acid spin labels containing the nitroxide group at either the C-5 position (5-SASL) or the C-16 position (16-SASL). Before incorporation into SR, these labels were diluted from a 0.1 M dimethylformamide stock solution into ethanol (because of the greater miscibility of ethanol with water). A sufficient amount of label was added to SR to provide a ratio of 1 label per 150 phospholipids, while keeping the final ethanol concentration in all samples below 1%. The labeled SR was vortexed well, diluted by a factor of 10 with experimental buffer, and pelleted in a low-speed table-top centrifuge to remove any unbound label. The pellet was resuspended in the experimental buffer to approximately 25 mg/ml and transferred to a 50-μl glass capillary in preparation for EPR spectral acquisition.

Phospholamban phosphorylation

Before our experiments, the SR membranes were treated with type 2A protein phosphatase at room temperature for 30 min to ensure complete dephosphorylation of PLB (Jones and Field, 1993). PLB phosphorylation was performed just before gel electrophoresis and TPA data collection. SR vesicles were incubated with 40 μg/ml of the catalytic subunit of protein kinase-A in a buffer containing 50 mM Tris-HCl, 0.1 mM DTT, 2 mM $MgCl_2$, 0.75 mM ATP containing 2–3 mCi/ml [γ-^{32}P]ATP, 50 nM phosphatase inhibitor calyculin A, pH 7.0, at 30°C. After a 3-min incubation, the sample was immediately centrifuged at 100,000 × g_{max} for 5 min at 4°C, and the phosphorylated SR vesicles were resuspended in ice-cold 30 mM MOPS, 250 mM sucrose, 50 nM calyculin A, pH 7.0, and kept on ice. Control SR was treated in the same way, except that protein kinase-A was omitted.

The specificity of PLB phosphorylation was measured by autoradiography of SDS gels of sample aliquots taken directly from the PLB phosphorylation medium and spectroscopy samples (Voss et al., 1994). Fig. 2 indicates that most of the phosphorylation was localized to the PLB protein. This assignment was confirmed by comparison of the autoradiographs of SR

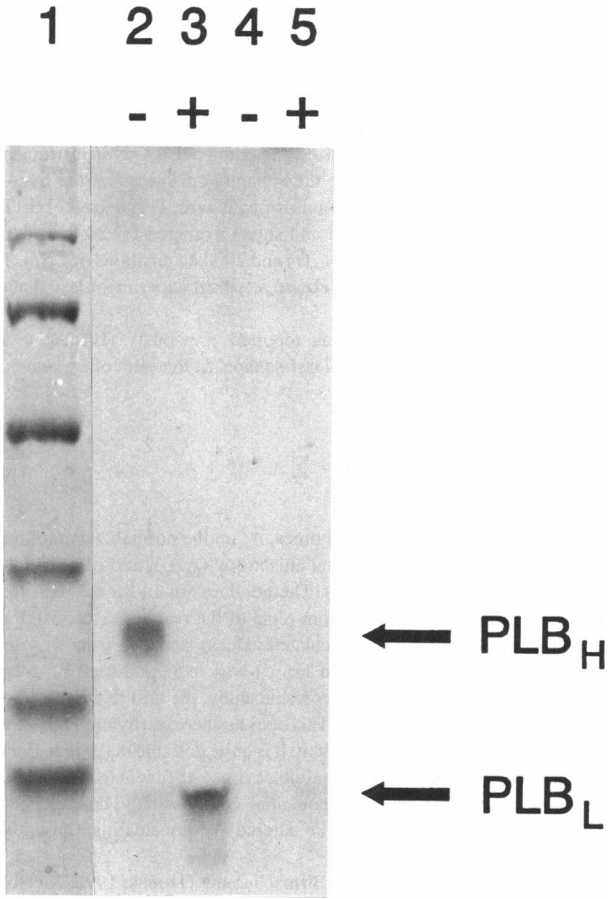

FIGURE 2 Autoradiograph depicting phosphorylation of PLB by the catalytic subunit of cAMP-dependent protein kinase. Lane 1 shows Coomassie blue-stained protein molecular mass standards, as defined in Fig. 1. Lanes 2 and 3 are mouse ventricular SR, and lanes 4 and 5 are mouse atrial SR. PLB was phosphorylated as described in Materials and Methods. The ± symbols indicate whether the membrane samples were boiled in SDS before electrophoresis. PLB_H and PLB_L denote the pentameric and monomeric forms of PLB, respectively.

samples analyzed before (denoted by – in Fig. 2) and after (denoted by + in Fig. 2) boiling in SDS, which converts PLB pentamers running at ~25 kDa (designated PLB_H) into PLB monomers running at about 6 kDa (designated PLB_L). The level of PLB phosphorylation was determined by excising regions on the gel corresponding to the exposed regions on the autoradiograph and placing these samples in scintillation vials for liquid scintillation counting. Four separate measurements of PLB phosphorylation in mouse ventricular SR resulted in an average of 0.51 ± 0.08 nmol phosphate/mg SR protein. No PLB phosphorylation in the atrial tumor SR vesicles was discernible above the background.

Time-resolved phosphorescence anisotropy spectroscopy

The experimental and analytical procedures for time-resolved phosphorescence anisotropy (TPA) of skeletal and cardiac SR have been described in detail previously (Birmachu and Thomas, 1990; Birmachu et al., 1993). Before TPA data collection, oxygen was removed enzymatically from the labeled sample (0.2 to 0.4 mg SR/ml) in a sealed 1-cm quartz cuvette with 100 μg/ml glucose oxidase, 15 μg/ml catalase, and 5 mg/ml glucose for 10–15 min, as described previously (Birmachu et al., 1993). The spectrometer used to obtain TPA decays was described previously (Ludescher and Thomas, 1988). The phosphorescence anisotropy (r) is given by

$$r(t) = \frac{I_{vv} - GI_{vh}}{I_{vv} + 2GI_{vh}}, \tag{1}$$

where I_{vv} and I_{vh} are the time-dependent decays of the phosphorescence intensities observed through polarizers oriented parallel and perpendicular, respectively, to the vertically polarized excitation pulse. G is an instrumental correction factor determined from the apparent anisotropy of the free dye in solution, for which the corrected anisotropy is zero. TPA decays of ErITC-labeled Ca-ATPase were detected and signal-averaged for 20 loops, each consisting of 2000 acquisitions of $I_{vv}(t)$ and 2000 acquisitions of $I_{vh}(t)$. The laser repetition rate was 100–200 Hz, so a typical experiment lasted about 10 min.

TPA decays were analyzed as reported previously (Birmachu and Thomas, 1990), using a nonlinear least-squares fit to a sum of exponentials plus a constant:

$$\frac{r(t)}{r(0)} = A(t) = \sum_{i=1}^{n} A_i e^{-t/\phi_i} + A_\infty, \tag{2}$$

where ϕ_i are rotational correlation times, A_i are the normalized amplitudes (r_i/r_0), A_∞ is the normalized residual anisotropy (r_∞/r_0), and r_0 is the initial anisotropy ($r(0) = r_0 = \Sigma r_i + r_\infty$). The goodness-of-fit for the anisotropy decays was evaluated primarily from plots of the residuals (the difference between the measured and the calculated values), and also from χ^2 values. The number of exponentials (n in Eq. 2) was increased until no further improvement was observed. In the present study, the best fit for anisotropy decays was consistently for $n = 3$. This does not necessarily imply that there are precisely three components present. It is quite possible that either 1) there are more than three species but signal/noise is not sufficient to resolve them, or 2) there is a continuum of exponential components. The conclusions of the present study would not be altered by considering these other alternatives.

It has been shown previously (Birmachu and Thomas, 1990; Mersol et al., 1995) that the TPA of ErITC-SR is dominated by the uniaxial rotation of the labeled Ca-ATPase about an axis normal to the bilayer. For this model, each different rotational diffusion coefficient should give rise to a biexponential decay component (Kinosita et al., 1984) (reviewed by Thomas, 1986), but it has been shown that a single-exponential approximation is sufficient to describe the decay for each rotating species in ErITC-SR (Birmachu and Thomas, 1990; Mersol et al., 1995). As long as the probe orientation relative to the protein is the same for all proteins, the mole fraction (f_i) of probes in the ith rotating species, having rotational correlation time ϕ_i is given by

$$f_i = \frac{A_i}{1 - A_{\infty 0}}, \; f_I = \frac{(A_\infty - A_{\infty 0})}{(1 - A_{\infty 0})}, \tag{3}$$

where f_I is the fraction of probes (i.e., proteins) that are immobile on the time scale of the experiment (Birmachu et al., 1993). A_∞ is the normalized residual anisotropy of a reference sample for which $f_I = 0$ and describes the extent to which the probe's motion is restricted in angular range, due to the fixed angles θ_{ma}, and θ_{me} of the probe's absorption and emission transition moments relative to the membrane normal:

$$A_{\infty 0} = \frac{P_2(\cos\theta_{ma})\, P_2(\cos\theta_{me})}{P_2(\cos\theta_{ae})}, \tag{4}$$

where $P_2(x) = (3x^2 - 1)/2$, and θ_{ae} is the angle between the absorption and emission transition moments (Lipari and Szabo, 1980). $A_{\infty 0}$ has been shown to be 0.22 for ErITC-Ca-ATPase in skeletal SR (Birmachu and Thomas, 1990) and is assumed to be the same for cardiac SR (Birmachu et al., 1993). If this value of $A_{\infty 0}$ is an underestimate, it would result in an underestimate of f_i and an overestimate of f_I (Eq. 3).

The rotational diffusion coefficient (D_m) for uniaxial rotation of a cylindrical membrane protein can be expressed as a function of the membrane lipid viscosity (η), the temperature (T), and the effective radius (a) of the portion of the protein in the bilayer (Saffman and Delbrück, 1975):

$$D_m = \frac{kT}{4\pi a^2 h\eta} \propto \frac{1}{\phi}, \tag{5}$$

where h is the thickness of the hydrocarbon phase of the lipid bilayer. Thus, the rotational correlation time (inversely proportional to the diffusion coefficient), should be proportional to the lipid viscosity (inverse of fluidity) and to the intramembrane cross-sectional area (πa^2) of the rotating protein. This theory relating protein size and lipid fluidity to protein rotational mobility is supported by previous studies on the Ca-ATPase as measured by both ST-EPR (Squier et al., 1988a, b) and phosphorescence anisotropy (Birmachu and Thomas, 1990), which showed that the microsecond rotational motions of the SR probes used in those studies (including ErITC) are dominated by the uniaxial rotation of the Ca-ATPase, not by rotations within the Ca-ATPase or by tumbling of the membrane vesicles. If there are no changes in lipid viscosity, any PLB-dependent changes in the observed rotational correlation times must be due to changes in the effective radius (a in Eq. 5) of the rotating protein. The only plausible source of large changes in protein size in SR is protein association into different sized oligomers, with the rotational correlation time ϕ_i roughly proportional to the size of the oligomer (Birmachu and Thomas, 1990). Thus, the distribution of oligomeric species is given by the fractions f_i (Eq. 3). The fraction of proteins in immobile species f_I, determined from the residual anisotropy A_∞, thus corresponds to protein aggregates so large that they undergo little or no rotational diffusion in the 1-ms time window of the TPA experiment. Because the correlation time of a Ca-ATPase monomer or dimer is on the order of 5–30 μs, these immobile aggregates must contain more than 10 Ca-ATPase molecules (Birmachu and Thomas, 1990; Voss et al., 1991; Birmachu et al., 1993).

EPR spectroscopy

EPR spectra were acquired with a Bruker ESP-300 spectrometer equipped with a Bruker ER4201 cavity, and digitized with the spectrometer's built-in microcomputer using Bruker OS-9-compatible ESP 1620 spectral acquisition software. Spectra were downloaded to an IBM-compatible microcomputer and analyzed with software developed in our laboratory by R. L. H. Bennett. EPR spectra were obtained using 100-kHz field modulation (with a peak-to-peak modulation amplitude of 2 Gauss), with a microwave field intensity (H_1) of 0.14 Gauss (Squier and Thomas, 1986). Sample temperature was controlled to within 0.5°C with a Bruker ER 4111VT-1003 variable temperature controller. Sample temperature was monitored with a Sensortek

Bat-21 digital thermometer using an IT-21 thermocouple probe inserted into the top of the sample capillary, such that it did not interfere with spectral acquisition.

EPR spectra were analyzed by measuring the inner ($2T'_\perp$) and outer ($2T'_\parallel$) spectral splittings, which are sensitive mainly to the label's rotational amplitude, and the half-width at half-height of the low-field peak (Δ_L), which is sensitive mainly to the label's rate of motion (Fig. 3). The effective order parameter (S) for the hydrocarbon chain mobility of 5- and 16-SASL was evaluated from the splittings by two equivalent methods. The 5-SASL spectra had well resolved extrema, such that both $2T'_\perp$ and $2T'_\parallel$ could be measured, allowing the use of the expression (Gaffney, 1976):

$$S = \frac{T'_\parallel - (T'_\perp + C)}{T'_\parallel + 2(T'_\perp + C)} \times 1.66 \quad (6)$$

where $C = 1.4 - 0.053(2T'_\parallel - 2T'_\perp)$. For 16-SASL spectra, Eq. 6 is not applicable for calculating the effective order parameter. Therefore, 16-SASL order parameters were determined by the expression (Gaffney, 1976):

$$S = \frac{T_o - T'_\perp}{T_o - T_\perp}, \quad (7)$$

where T_o is the isotropic hyperfine splitting constant in the absence of anisotropic effects and $T_\perp$ is the minimum principal value of the hyperfine constant for an axially symmetric system such as a lipid bilayer. The values of T_o and $T_\perp$ used in this study were 14.3 and 6.3 G, respectively, as determined previously (Squier and Thomas, 1989). The effective lipid fluidity (T/η) was calculated using the order parameter (S) obtained from the 5- or 16-SASL spectra using the following empirical expression (Squier et al., 1988a):

$$S = -0.42\left(\log\frac{T}{\eta}\right) + 0.56, \quad (8)$$

where T is the absolute temperature and η is the depth-dependent bilayer viscosity in centipoise. This fluidity parameter, along with Eq. 5, can be used to determine whether differences in Ca-ATPase rotational mobility in atrial versus ventricular SR are due to differences in bilayer fluidity (T/η) or to changes in the size (aggregation state) of the rotating proteins (Mahaney and Thomas, 1991; Voss et al., 1991).

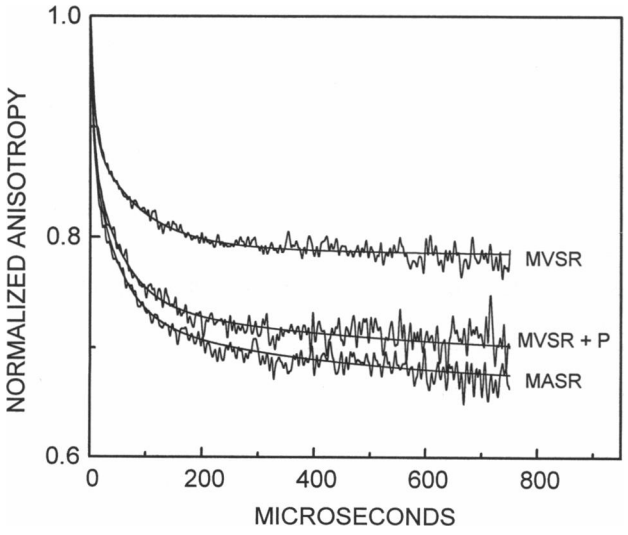

FIGURE 3 Phosphorescence anisotropy decay of ErITC-labeled Ca-ATPase in MVSR, mouse ventricular SR with PLB phosphorylation (MVSR + P), and MASR vesicles (0.3–0.6 mg/ml at 25°C in 60 mM KCl, 1 mM $MgCl_2$, 50 mM MOPS, pH 7.0). Overlayed on the decay curves are the fits to the decays using Eq. 2 and the parameters given in Table 2.

RESULTS

Phosphorescence emission decay

The decay of the total unpolarized phosphorescence emission intensity of mouse atrial tumor SR and mouse ventricular SR labeled with ErITC was multiexponential (Table 1). The emission decay from both preparations was best fit by a four-exponential function, with no improvement in the residual or X^2 of the fit by increasing n to 5. The similarities of each lifetime and amplitude in each system is consistent with our finding the same specificity of labeling determined from gel electrophoresis. Thus, differences in the anisotropy decay are not attributed to different lifetime components or component amplitudes.

Phosphorescence anisotropy

The TPA decays of ErITC-Ca-ATPase in the two SR preparations are shown in Fig. 3. As shown previously for the TPA decay of ErITC-labeled Ca-ATPase (Birmachu and Thomas, 1990), the TPA decays for ErITC-mouse ventricular SR were best fit to a three-exponential decay function (Table 2). The Ca-ATPase in both atrial tumor and ventricular SR exhibits rotational correlation times that are identical within experimental error (Table 2). The major difference between the two SR sources is in the normalized residual anisotropy, A_∞, which is significantly higher in mouse ventricular SR (0.784 ± 0.006) than in mouse atrial tumor SR (0.664 ± 0.011), suggesting a greater degree of motional restriction of the ATPase in ventricular SR. Phosphorylation of PLB reduced the A_∞ value of ventricular SR to 0.692 ± 0.008, a level close to that of the PLB-deficient atrial tumor SR, consistent with a model of PLB-induced protein association and Ca-ATPase inhibition. In contrast, exposing MASR to phosphorylating conditions did not affect the TPA decay curve of this sample.

Lipid chain dynamics

To determine whether higher membrane viscosity could account for the decreased Ca-ATPase rotational mobility in ventricular SR, we measured the lipid hydrocarbon chain mobility in mouse ventricular SR and mouse atrial tumor SR using stearic acid spin labels. 5-SASL was used to measure chain dynamics near the head group region of the bilayer, and 16-SASL was used to measure chain dynamics near the central region of the bilayer. Typical EPR spectra obtained from each probe in mouse ventricular SR and mouse atrial tumor SR are shown in Fig. 4. The spectra were characterized by the outer splitting, $2T'_\parallel$, inner splitting, $2T'_\perp$, the outer half-width at half-height of the low-field peak, Δ_L, the order parameter of the label, S, and the bilayer fluidity at the label depth, T/η (Table 3). Because sample limitations, each experiment was performed only once, and typical errors in the spectral parameters (estimated from Mahaney and Thomas, 1991; and Mahaney et al., 1992) are listed in the legend of Table 3. The mobility of the lipid hydrocarbon chains in the

TABLE 1 Total phosphorescence emission decay parameters for mouse ventricular and atrial tumor SR labeled with erythrosin-5-isothiocyanate

Sample	τ_1	τ_2	τ_3	τ_4	A_1	A_2	A_3	A_4
Atrial tumor SR								
	11	38	129	383	0.219	0.222	0.236	0.323
	(1)	(3)	(9)	(11)	(0.007)	(0.013)	(0.004)	(0.018)
Ventricular SR								
	10	31	117	385	0.289	0.184	0.214	0.313
	(1)	(2)	(5)	(3)	(0.013)	(0.004)	(0.002)	(0.011)

Phosphorescence lifetimes, τ_i (in μs), were obtained from a nonlinear least-squares fit of the total (unpolarized) phosphorescence intensity decays of ErITC attached to the Ca-ATPase. The data were fit to:

$$\frac{I(t)}{I(0)} = \sum_{i=1}^{n} A_i e^{-t/\tau_i} + A_\infty$$

using $n = 4$, with χ^2 from all fits within the range of 2.40–2.67. τ_i are the triplet excited state lifetimes with fractional contributions A_i (normalized to the initial intensity). The values are averages of four experiments. Values in parentheses are the SDs.

mouse atrial tumor SR bilayer is only slightly restricted relative to that of the mouse ventricular SR bilayer, as evidenced by the very small changes in the splittings of the 5- and 16-SASL spectra (~1 and 3% change in $2T'_\parallel$ and $2T'_\perp$, respectively, for each label). These small differences in splittings translated into slightly larger reductions of the order parameter (3.2 and 3.8% for the 5- and 16-SASL spectra, respectively) and fluidity (7.5 and 5.4% for the 5- and 16-SASL spectra, respectively) in mouse atrial tumor SR relative to mouse ventricular SR. Given the estimated limits of error on each of the spectral parameters, these differences may not be significant, such that there is no difference in the lipid hydrocarbon chain mobility in the two bilayers. Nevertheless, because the fluidity of the mouse atrial tumor SR bilayer is slightly *reduced* relative to that of the mouse ventricular SR bilayer, the increased Ca-ATPase mobility in mouse atrial tumor SR versus mouse ventricular SR cannot be attributed to differences in lipid fluidity.

DISCUSSION

Summary of results

We present here the first direct comparative study of the Ca-ATPase rotational dynamics in native cardiac SR membranes with and without the regulatory protein PLB, designed to elucidate the underlying mechanism for the regulation of the cardiac Ca-ATPase. The Ca-ATPase of mouse ventricular SR, which contains PLB, and mouse atrial tumor SR, which is essentially devoid of PLB, was labeled with ErITC with similar specificity in both SR preparations. TPA measurements showed that ventricular Ca-ATPase is less rotationally mobile than the atrial Ca-ATPase. The difference in the motional properties of the Ca-ATPases in the two SR preparations is due primarily to differences in the amplitudes of motion, especially the limiting anisotropy A_∞, not in the rate ($1/\phi$) of motion. Conventional EPR spectra of spin-labeled fatty acids showed no significant difference in lipid bilayer fluidity in the two SR preparations.

Lipid dynamics

From the theory of transmembrane protein rotational mobility (Saffman and Delbrück, 1975) (Eq. 5 in the present study), the observed differences in Ca-ATPase mobility could be due to differences in either 1) membrane viscosity (η in Eq. 5), or 2) the average cross sectional area (πa^2 in Eq. 5) of the rotating units in the plane of the membrane (i.e., an increased state of protein association). The strong influence of SR membrane fluidity on Ca-ATPase rotational mobility has been demonstrated previously (Bigelow and Thomas, 1987; Squier et al., 1988a). Therefore, we measured the lipid chain dynamics (Fig. 4, Table 3) to determine

TABLE 2 Phosphorescence anisotropy decay parameters for mouse ventricular and atrial Ca-ATPase labeled with ErITC

Sample	ϕ_1	ϕ_2	ϕ_3	A_1	A_2	A_3	A_∞	r_0
Atrial tumor SR								
	5	50	440	0.120	0.151	0.064	0.664	0.101
	(1)	(2)	(20)	(0.016)	(0.018)	(0.008)	(0.011)	(0.004)
Ventricular SR								
	6.5	83	457	0.110	0.098	0.009	0.784	0.102
	(2)	(13)	(17)	(0.008)	(0.011)	(0.003)	(0.006)	(0.002)
Phosphorylated ventricular SR								
	5.5	53	478	0.120	0.137	0.051	0.692	0.104
	(1)	(2)	(48)	(0.006)	(0.020)	(0.014)	(0.008)	(0.003)

Phosphorescence anisotropy parameters obtained from a nonlinear least squares analysis (Eq. 2 in Materials and Methods) of phosphorescence anisotropy decays of ErITC-SR. ϕ_i are the rotational correlation times, and A_i are the amplitudes normalized to r_0. r_0 is the fit value of the anisotropy extrapolated to zero time, and $A_\infty = r_\infty/r_0$ is the normalized residual anisotropy. The values are averages of four experiments. Values in parentheses are the SDs. χ^2 from fits with Eq. 2 in Materials and Methods of all data sets ranged from 1.43 to 1.63 for $n = 3$.

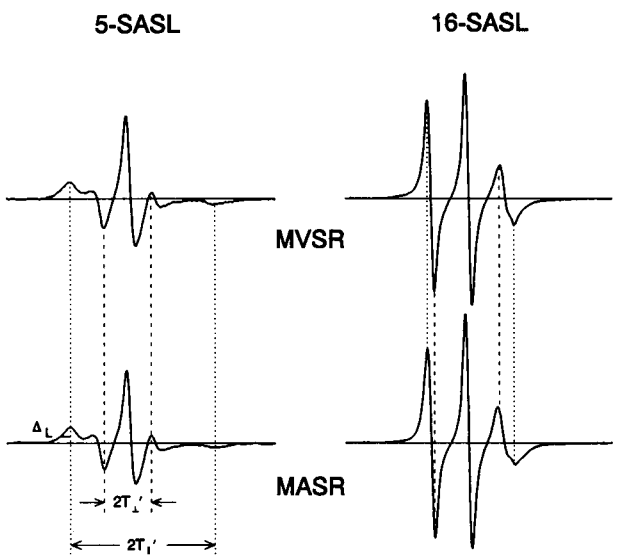

FIGURE 4 EPR spectra of stearic acid spin probes at different bilayer depths in MVSR and MASR vesicles obtained at 25°C. Samples were prepared for EPR analysis as described in Materials and Methods. Spectra of 5-SASL (*left*) and 16-SASL (*right*) report lipid hydrocarbon chain fluidity near the headgroup and central region of the bilayer, respectively. Spectra were characterized by the outer ($2T_\parallel'$) and inner ($2T_\perp'$) spectral splittings, and the half-width at half-height of the low field peak (Δ_L). Baselines represent 100 Gauss.

TABLE 3 5- and 16-SASL EPR spectral parameters at 25°C

	Mouse ventricular SR	Mouse atrial tumor SR
5-SASL		
$2T_\parallel'$	53.9 G	54.3 G
$2T_\perp'$	18.0 G	17.7 G
Δ_L	3.4 G	3.1 G
S	0.63	0.65
T/η	0.67 K/cP	0.62 K/cP
16-SASL		
$2T_\parallel'$	32.9 G	33.2 G
$2T_\perp'$	24.5 G	23.6 G
Δ_L	1.5 G	1.7 G
S	0.26	0.27
T/η	5.18 K/cP	4.90 K/cP

Conventional EPR parameters: outer splitting, $2T_\parallel'$; inner splitting, $2T_\perp'$; outer half-width at half-height of the low-field peak, Δ_L; order parameter, S; bilayer fluidity, T/η. Parameters $2T_\parallel'$, $2T_\perp'$, and Δ_L, in Gauss, are defined in Fig. 4. Order parameters are calculated from the splitting values using Eqs. 1 and 2. Bilayer fluidities (K/centipoise) are calculated from the order parameters using Eq. 3. Values correspond to a single measurement, where typical repetition errors are: $2T_\parallel'$ and $2T_\perp'$, ±0.5 G; Δ_L, ±0.2 G; S, ±0.01, 5-SASL T/η, ±0.03 K/cP; 16-SASL T/η, ±0.1. Mouse ventricular SR and mouse atrial tumor SR correspond to mouse ventricular and atrial tumor SR, respectively.

whether any significant difference in the lipid character could account for the difference in protein dynamics. A direct measurement of the bilayer fluidity (T/η) provides direct information on the predicted effect of the lipid environment on protein rotational mobility. The bilayer fluidity at both the headgroup region (measured by 5-SASL) and the bilayer center (measured by 16-SASL) were indistinguishable in ventricular and atrial tumor SR (Table 3). Because Eq. 5 predicts the rotational diffusion coefficient (D_m) of a membrane protein to be directly proportional to lipid fluidity (T/η), the large differences in the Ca-ATPase rotational dynamics cannot be explained by the negligible differences in membrane viscosity. Thus, *the difference in protein dynamics most likely results from the differences in protein associations.*

Protein dynamics

The best fit using Eq. 2 to the TPA decays of both ventricular and atrial ErITC-SR was achieved with $n = 3$, consistent with previous results from this laboratory (Voss et al., 1994; Birmachu et al., 1993; Birmachu and Thomas, 1990; Voss et al., 1991). It has been shown previously that the TPA decay of ErITC-SR reports primarily the uniaxial diffusion of the Ca-ATPase; that is, the rotation of the protein about the membrane normal (Cherry, 1978), as predicted by Eqs. 3–5 (Birmachu and Thomas, 1990). Each correlation time (ϕ_i, Eq. 2) is proportional to the bilayer viscosity (η in Eq. 5) and to the cross sectional area of the protein in the membrane plane (πa^2 in Eq. 5) for the ith rotating species (monomer, dimer, etc.), and each pre-exponential factor (amplitude A_i in Eq. 2) is proportional to the mole fraction of Ca-ATPase molecules in that species. The primary difference between the mouse atrial and ventricular TPA decays is in the pre-exponential factors A_i, not in the correlation times ϕ_i (Table 2). We have previously discussed in detail that ϕ_2 and ϕ_3 can be assigned to represent small and intermediate aggregation states of the Ca-ATPase, respectively (Voss et al., 1991; Birmachu and Thomas, 1990). The greatest ambiguity is with ϕ_1, which could be assigned as a resolved monomer or segmental motion of the protein backbone.

The most striking difference in the phosphorescence anisotropy decay between ventricular and atrial tumor SR ATPases is the difference in the magnitude of A_∞, representative of the species whose motion is too slow to observe on the time scale of the TPA experiment. There are three possible explanations for this difference. First, the Ca-ATPase in mouse ventricular SR could have a smaller amplitude of wobble (cone angle θ_c) for rotation about axes in the membrane plane, but this is unlikely, because the rotation of the skeletal Ca-ATPase is dominated by uniaxial diffusion, not wobble (Birmachu and Thomas, 1990). Second, the two systems could differ in the orientation of the probe relative to the protein's axis of rotation (the membrane normal) in uniaxial diffusion (Eq. 4). Although this cannot be ruled out, it is unlikely, because 1) the enzymes are of identical sequence, predicting identical topology, 2) a previous comparison of cardiac and skeletal SR (which lacks PLB) using ST-EPR of a probe attached to a different site gives qualitatively the same answer in terms of overall mobility, and 3) the difference in A_∞ can be explained more simply without invoking this conformational change. The third and most likely explanation for the larger A_∞ in ventricular SR is an *increased fraction of proteins rotating on a time scale slower than the window of spectroscopic detection* (in this case, 1 ms). As discussed earlier, this cannot be due to greater lipid

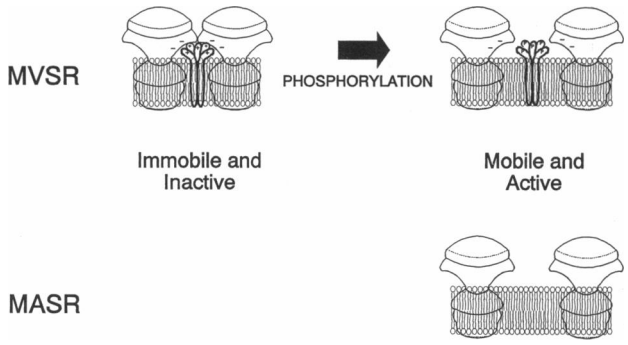

FIGURE 5 Model for PLB-dependent inhibition of the Ca-ATPase. Mouse atrial SR contains negligible amounts of PLB, so the Ca-ATPase has increased rotational mobility and activity. Unphosphorylated PLB in MVSR decreases Ca-ATPase rotational mobility by increasing large-scale ATPase aggregation, with concomitant reduction of enzymatic activity. Phosphorylation of PLB neutralizes the peptide's cytoplasmic basic (positive) charges, and thereby disrupts the electrostatic interaction between PLB and one or more negative charge clusters on the cytoplasmic domain of the enzyme. Mobilization of the Ca-ATPase relieves the inhibition. Although only two Ca-ATPase molecules are shown, large-scale aggregation involving 10 or more Ca-ATPase molecules may be required for inhibition.

viscosity (η in Eq. 5) in mouse ventricular SR, which would need to be larger by a factor of 10 or more in a discrete domain of the bilayer. This is clearly not consistent with the V_1 EPR measurements of lipid fluidity in ventricular and atrial tumor SR (Fig. 4, Table 3). Thus, the larger A_∞ in mouse ventricular SR is almost certainly due to a very large increase in the cross sectional area (πa^2 in Eq. 5) of the rotating body in the plane of the membrane, i.e., *to large-scale lateral association of the protein.*

The residual anisotropy value (A_∞) can be used to estimate the fraction of Ca-ATPase that is highly immobilized in large aggregates (Eq. 3, see Materials and Methods). We assume that these large aggregates are completely immobilized in our 1-ms time window of observation, such that their residual anisotropy is equal to their initial anisotropy ($A_\infty = A_0 = 1$). We also assume that enzymes not in large aggregates have the same A_∞ (0.22) as observed in skeletal SR (Birmachu and Thomas, 1990). Thus, the observed residual anisotropy in mouse ventricular ($A_\infty = 0.78$), phosphorylated ventricular ($A_\infty = 0.69$) and atrial ($A_\infty = 0.66$) SR, is consistent with 72, 60, and 56% of the enzyme in a highly aggregated state, respectively. Consistent with the hypothesis that increased Ca-ATPase association correlates with decreased enzyme activity, both the absence of PLB in atrial SR or phosphorylation of PLB in ventricular SR results in activation of calcium transport (Jones and Field, 1993) and a decrease in the fraction of large-scale Ca-ATPase aggregates. The high level of Ca-ATPase immobilization in mouse cardiac SR that is independent of the presence of PLB can most likely be attributed to the fraction of highly aggregated Ca-ATPase in this system (see *Labeling and Sample Preparation* in Materials and Methods). The nature of the aggregation and the likely functional manifestations warrant further study.

Relationship to other work

We have demonstrated previously that nearly half of the Ca-ATPase in dog cardiac SR exists as large-scale aggregates, compared with effectively no large-scale Ca-ATPase aggregates in fast-twitch skeletal SR (Birmachu et al., 1993). We have also shown that phosphorylation of PLB in dog cardiac SR promotes Ca-ATPase disaggregation and increases Ca-transport rates (Voss et al., 1994). In the present study, we find that the Ca-ATPase of mouse ventricular SR is less rotationally mobile than the Ca-ATPase of mouse atrial tumor SR, because of a larger fraction of ATPases in large-scale aggregates. The primary distinction in protein components between mouse ventricular and atrial SR is the absence of PLB in the latter. Thus, inhibition of Ca-ATPase activity by PLB strongly correlates with a PLB-dependent increase in the level of large-scale Ca-ATPase association.

CONCLUSION

We have proposed previously a model for the physical basis of PLB inhibition of the Ca-ATPase (Voss et al., 1994; Birmachu et al., 1993). In this model, the basic cytoplasmic charges of a phospholamban pentamer interact with two or more Ca-ATPase molecules via the acidic stalk region. Based on previous model studies of the interaction of a basic amphipathic peptide with the Ca-ATPase (Voss et al., 1991; Mahaney and Thomas, 1991; Mahaney et al., 1992), such interaction would lead to a large network of immobilized Ca-ATPase proteins, consistent with our spectroscopic results. The Ca-ATPase in atrial SR, lacking phospholamban, would therefore display greater mobility, also consistent with our spectroscopic results (Fig. 5). Further work will be needed to determine the molecular mechanism whereby 1) PLB aggregates the Ca-ATPase in a phosphorylation-dependent manner, and 2) this aggregation inhibits the Ca-ATPase at low calcium.

This work was supported by grants from the American Heart Association, Minnesota Affiliate, to D.D.T. and J.E.M., and National Institutes of Health grants to D.D.T. (GM27906) and to L.R.J. (HL49428 and HL28556).

REFERENCES

Autry, J. M., S. E. Cala, B. T. Scott, and L. R. Jones. 1994. Co-expression of SERCA2a and phospholamban with functional coupling in SF21 cells. *Biophys. J.* 66:216*a*. (Abstr.)

Bigelow, D. J., and D. D. Thomas. 1987. Rotational dynamics of lipid and the Ca-ATPase in sarcoplasmic reticulum: the molecular basis of activation by diethyl ether. *J. Biol. Chem.* 262:13449–13456.

Birmachu, W., and D. D. Thomas. 1990. Rotational dynamics of the Ca-ATPase in sarcoplasmic reticulum studied by time-resolved phosphorescence anisotropy. *Biochemistry.* 29:3904–3914.

Birmachu, W., J. C. Voss, C. F. Louis, and D. D. Thomas. 1993. Protein and lipid rotational dynamics in cardiac and skeletal sarcoplasmic reticulum detected by EPR and phosphorescence anisotropy. *Biochemistry.* 32:9445–9453.

Cherry, R. J. 1978. Measurement of protein rotational diffusion in membranes by flash photolysis. *Methods Enzymol.* 54:47–61.

Chiesi, M., and R. Schwaller. 1989. Involvement of electrostatic phenomena in phospholamban-induced stimulation of Ca uptake into cardiac sarcoplasmic reticulum. *FEBS Lett.* 244:241–244.

Davis, B., A. Schwartz, F. Samaha, and E. G. Kranias. 1983. Regulation of cardiac sarcoplasmic reticulum calcium transport by calcium-calmodulin-dependent phosphorylation. *J. Biol. Chem.* 258:13587–13591.

Fabiato, A. 1988. Computer programs for calculating total from specified free or free from specified total ionic concentrations in aqueous solutions containing multiple metals and ligands. *Methods Enzymol.* 157:378–417.

Field, L. J. 1988. Atrial natriuretic factor-SV40 T antigen transgenes produce tumors and cardiac arrhythmias in mice. *Science.* 239:1029–1033.

Fujii, J., K. Maruyama, M. Tada, and D. H. Maclennan. 1990. Co-expression of slow-twitch/cardiac muscle Ca^{2+}-ATPase (SERCA2) and phospholamban. *FEBS Lett.* 273:232–234.

Fujii, J., A. Ueno, K. Kitano, S. Tanaka, M. Kadoma, and M. Tada. 1987. Complete complementary DNA-derived amino acid sequence of canine cardiac phospholamban. *J. Clin. Invest.* 79:301–304.

Gaffney, B. J. 1976. Spin Labeling Theory and Practice. L. J. Berliner, editor. Academic Press, New York. 567–571.

Inesi, G. 1985. Mechanism of calcium transport. *Annu. Rev. Physiol.* 47: 573–601.

Inui, M., B. K. Chamberlain, A. Saito, and S. Fleischer. 1986. The nature of the modulation of Ca^{2+} transport as studied by reconstitution of cardiac sarcoplasmic reticulum. *J. Biol. Chem.* 261:1794–1800.

Jones, L. R., and S. E. Cala. 1981. Biochemical evidence for functional heterogeneity of cardiac sarcoplasmic reticulum vesicles. *J. Biol. Chem.* 256:11809–11818.

Jones, L. R., and L. J. Field. 1993. Residues 2–25 of phospholamban are insufficient to inhibit the Ca^{2+} transport ATPase of cardiac sarcoplasmic reticulum. *J. Biol. Chem.* 268:11486–11488.

Jones, L. R., H. K. Simmerman, W. W. Wilson, F. Gurd, and A. D. Wegener. 1985. Purification and characterization of phospholamban for canine cardiac sarcoplasmic reticulum. *J. Biol. Chem.* 260:7721–7730.

Jorgensen, A. O., and L. R. Jones. 1986. Localization of phospholamban in slow but not fast canine skeletal muscle fibers. *J. Biol. Chem.* 261:3375–3781.

Karon, B. S., and D. D. Thomas. 1993. Molecular mechanism of Ca^{2+}-ATPase activation by halothane in sarcoplasmic reticulum. *Biochemistry.* 32:7503–7511.

Kinosita, K., S. Ishiwata, H. Yoshimura, H. Asai, and A. Ikegami. 1984. Submicrosecond and microsecond rotational motions of myosin head in solution and in myosin synthetic filaments as revealed by time-resolved optical anisotropy decay measurements. *Biochemistry.* 23:5963–5975.

Kirchberger, M. A., and M. Tada. 1976. Effects of adenosine 3′:5′-monophosphate-dependent protein kinase on sarcoplasmic reticulum isolated from cardiac, slow-and fast-contracting skeletal muscles. *J. Biol. Chem.* 251:725–729.

Kirchberger, M. A., D. Borchman, and C. Kasinathan. 1986. Proteolytic activation of the canine cardiac sarcoplasmic reticulum calcium pumps. *Biochemistry.* 25:5484–5492.

Lipari, G., and A. Szabo. 1980. Effect of librational motion on fluorescence depolarization and nuclear magnetic resonance relaxation in macromolecules and membranes. *Biophys. J.* 30:489–506.

Lowry, O. H., N. J. Rosebrough, A. L. Farr, and R. J. Randall. 1951. Protein measurement with folin phenol reagent. *J. Biol. Chem.* 193:265–275.

Ludescher, R. D., and D. D. Thomas. 1988. Microsecond rotational dynamics of phosphorescent-labeled muscle cross-bridges. *Biochemistry.* 27:3343–3351.

Mahaney, J. E., and D. D. Thomas. 1991. Effects of melittin on molecular dynamics and Ca-ATPase activity in sarcoplasmic reticulum membranes: electron paramagnetic resonance. *Biochemistry.* 30:7171–7180.

Mahaney, J. E., J. Kleinschmidt, D. Marsh, and D. D. Thomas. 1992. Effects of melittin on lipid-protein interactions in sarcoplasmic reticulum membranes. *Biophys. J.* 63:1513–1522.

Manalan, A. S., and L. R. Jones. 1982. Characterization of the intrinsic cAMP-dependent protein kinase activity and endogenous substrates in highly purified cardiac sarcolemmal vesicles. *J. Biol. Chem.* 257: 10052–10062.

Mersol, J. V., J. E. Mahaney, H. Kutchai, and D. D. Thomas. 1995. Self-association accompanies inhibition of Ca-ATPase by thapsigargin. *Biophys. J.* 68:208–215.

Mitchinson, C., A. F. Wilderspin, B. J. Trinnaman, and N. M. Green. 1982. Identification of a labelled peptide after stoichiometric reaction of fluorescein isothiocyanate with the Ca^{2+}-dependent adenosine triphosphatase of sarcoplasmic reticulum. *FEBS Lett.* 146:87–92.

Saffman, P. J., and M. Delbruck. 1975. Brownian motion in biological membrane. *Proc. Natl. Acad. Sci. USA.* 79:4317–4321.

Simmerman, H. K. B., J. H. Collins, J. L. Theibert, A. D. Wegener, and L. R. Jones. 1986. Sequence analysis of phospholamban. *J. Biol. Chem.* 261:13333–13341.

Squier, T. C., and D. D. Thomas. 1986. Methodology for increased precision in saturation-transfer electron paramagnetic resonance studies of rotational dynamics. *Biophys. J.* 49:921–935.

Squier, T. C., and D. D. Thomas. 1988. Relationship between protein rotational dynamics and phosphoenzyme decomposition in the sarcoplasmic reticulum Ca-ATPase. *J. Biol. Chem.* 263:9171–9177.

Squier, T. C., and D. D. Thomas. 1989. Selective detection of the rotational dynamics of the protein-associated lipid hydrocarbon chains in sarcoplasmic reticulum membranes. *Biophys. J.* 56:735–748.

Squier, T. C., D. J. Bigelow, and D. D. Thomas. 1988a. Lipid fluidity directly modulates the overall protein rotational mobility of the Ca-ATPase in sarcoplasmic reticulum. *J. Biol. Chem.* 263:9178–9186.

Squier, T. C., S. E. Hughes, and D. D. Thomas. 1988b. Rotational dynamics and protein-protein interactions in the Ca-ATPase mechanism. *J. Biol. Chem.* 263:9162–9170.

Tada, M., and A. M. Katz. 1982. Phosphorylation of the sarcoplasmic reticulum and sarcolemma. *Annu. Rev. Physiol.* 44:401–423.

Tada, M., M. Kadoma, J. Fujii, Y. Kimura, and Y. Kijima. 1989. Molecular structure and function of phospholamban: the regulatory protein of calcium pump in cardiac sarcoplasmic reticulum. *Adv. Exp. Med. Biol.* 255: 79–89.

Tada, M., M. Kadoma, M. Inui, and J. Fujii. 1988. Regulation of Ca^{2+}-pump from cardiac sarcoplasmic reticulum. *Methods Enzymol.* 157:107–154.

Teruel, J. A., and G. Inesi. 1988. Roles of phosphorylation and nucleotide binding domains in calcium transport by sarcoplasmic reticulum adenosinetriphosphatase. *Biochemistry.* 27:5885–5890.

Thomas, D. D. 1986. Rotational diffusion of membrane proteins. *In* Techniques for Analysis of Membrane Proteins. R. Cherry and I. Ragan, editors. Chapman and Hall, London. 377–431.

Thomas, D. D., and B. S. Karon. 1994. Temperature dependence of molecular dynamics and calcium ATPase activity in sarcoplasmic reticulum. *In* The Temperature Adaptation of Biological Membranes. A. R. Cossins, editor. Portland Press, London. 1–12.

Thomas, D. D., and J. E. Mahaney. 1993. The functional effects of protein and lipid dynamics in sarcoplasmic reticulum. *In* Protein-Lipid Interactions. A. Watts, editor. Elsevier Science Publishers, North-Holland. 301–320.

Toyofuku, T., K. Kurzydlowski, M. Tada, and D. H. MacLennan. 1993. Identification of regions in the Ca^{2+}-ATPase of sarcoplasmic reticulum that affect functional association with phospholamban. *J. Biol. Chem.* 268:2809–2815.

Voss, J., W. Birmachu, D. M. Hussey, and D. D. Thomas. 1991. Effects of melittin on molecular dynamics and Ca-ATPase activity in sarcoplasmic reticulum membranes: time-resolved optical anisotropy. *Biochemistry.* 30:7498–7506.

Voss, J. C., L. R. Jones., and D. D. Thomas. 1994. The physical mechanism of calcium pump regulation in the heart. *Biophys. J.* 67:190–196.

Wegener, A. D., H. K. B. Simmerman, J. Liepnieks, and L. R. Jones. 1986. Proteolytic cleavage of phospholamban purified from canine cardiac sarcoplasmic reticulum vesicles. Generation of a low resolution model of phospholamban structure. *J. Biol. Chem.* 261:5154–5159.

Xu, Z., and M. A. Kirchberger. 1989. Modulation by polyelectrolytes of canine cardiac microsomal calcium uptake and the possible relationship to phospholamban. *J. Biol. Chem.* 264:16644–16651.